

B. COOLER EXPERIMENT PREPARATION

Introduction - H.O. Meyer

We are currently operating under the assumption that experimental research with the Cooler will begin in early 1988. In the beginning, the activity will be a mix between understanding the unexplored territory of the equilibrium interaction of stored, cooled beams with internal targets and a serious attempt to perform the nuclear physics measurements proposed for some of the early experiments.

Detailed planning for the startup phase of the Cooler experimental program has been in progress since December 1986. The currently accepted scenario calls for experiment CE-01 (see below) being ready to take data when the cooled beam becomes available and experiment CE-02 being close to this status. In order to make this goal compatible with our limited resources many parts of the detection equipment are being designed such that they can be shared by both experiments.

Aside from the first two experiments for which detailed planning is now in progress, a number of experiments have been proposed and presented to our Program Advisory Committee. Several of these are represented by outside users, a development we gladly welcome. Since one or more of these experiments may become active as early as late 1988 it is mandatory that planning for them starts now.

The usefulness of the Cooler as a nuclear physics research tool crucially depends on the availability of internal targets for a range of materials. Demands imposed by the cooling mechanism and other machine-related constraints require targets of unusual thicknesses. Supplying the Cooler experimenters with suitable targets thus represents a major development

task which is addressed by a dedicated research group instituted at IUCF within the past year.

Cooler Target Development - A. Berdoz, J. Doskow, W. Lozowski, H.-O. Meyer, H. Nann, D. Petasis and F. Sperisen

The effort level for the development of Cooler internal targets has greatly increased during 1986. Work is in progress on several approaches to targets, the maximum thickness of which is limited to the order of 100 ng/cm^2 or $10^{16} \text{ nuclei/cm}^2$.¹ Highest priority has been given a hydrogen gas target, to be used in the first Cooler experiment, CE-01.^{2,3} The ^{13}C -target, that is required for experiment CE-02,^{3,4} is expected to be either a microparticle beam ("dust gun") or in the form of very thin fibers or strips; so these options are pursued with second priority. Furthermore, the PAC has recommended feasibility tests for an experiment that calls for a ^6Li target, for which a promising scheme has been outlined in the proposal for this experiment.⁵ The actual development of such a target will begin as soon as a full-time person (e.g. graduate student) can be identified who is able to carry the responsibility for this project.

1. Gas Targets

The simplest approach to a gas target is to feed gas into a storage cell which has openings for the Cooler beam passing through.¹ While this scheme requires relatively little development effort, it suffers from the disadvantage of a fairly extended luminous volume (typically 10 cm long) and/or limited target thickness, and requires high pumping capacity. A much more elegant, but also technically more complex solution would be a supersonic jet⁶ which would provide a more localized and possibly also thicker target.

1.1. Storage Cell Gas Target

The maximum achievable target thickness depends critically on the optimization of the differential pumping system which is needed to evacuate gas leaving through the openings of the storage cell. In order to make sure that we understand the laws determining the gas flows in such systems, we have carried out some simple experiments at room temperature. In particular, we were interested in testing predictions for the molecular beam that is formed by the alignment of the differential pumping apertures along the beam axis. In the Cooler, this molecular beam will inevitably reach the vacuum chamber of the ring dipole magnet, resulting in an extra gas load there. Furthermore, we wanted to test gas flow rates in the intermediate flow regime, i.e. where the mean free path length is comparable to the diameter of the cell or its openings.

The experimental set-up for these tests is shown schematically in Fig. 4. Three vacuum chambers, making up a differential pumping system, were pumped each by a Balzers TPU 1500 turbo-molecular pump. Nitrogen or hydrogen was fed through a Vacuum General UltraFlo UC flow meter/controller into the cell located in the chamber to the left. The cell had apertures consisting of iris diaphragms that could be opened and closed with push-pull feed-throughs from outside the chamber. Iris diaphragms were also mounted on each side of the two tubes connecting the vacuum chambers (their aperture diameter could only be adjusted when the chamber was open). The target pressure, p_0 , or density, n_0 , was measured with an MKS Baratron, a capacitance sensor which has good accuracy between 1 and 10^{-4} Torr. Bayard-Alpert ion gauges were used to measure the pressure in each of the three vacuum chambers (Fig. 4). The two chambers to the right had metal seals throughout and had been moderately baked ($\approx 100^\circ\text{C}$), so

the background pressure p_3 (with no gas flow into the cell) was about $5 \cdot 10^{-10}$ Torr.

Figure 5 shows the measured and calculated p_0 (or n_0) as a function of the flow rate, Q_0 , into the cell, at aperture diameters of 8.5 mm. The agreement with the calculation, which is based on molecular flow condition, is within a few percent; there is only a slight deviation for N_2 above 10^{-2} Torr, where its mean free path length is $< 6.4\text{mm}$. The pressures p_1 , p_2 , and p_3 have been measured as a function of Q_0 at different aperture diameters. Results agree with the predictions

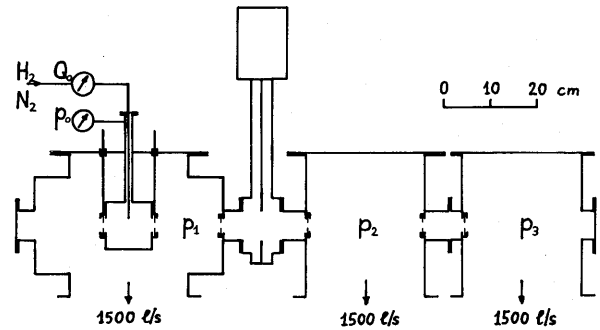


Figure 4. Schematic representation of the experimental arrangement used to study the gas flows through a storage cell and associated differential pumping system. See text for details.

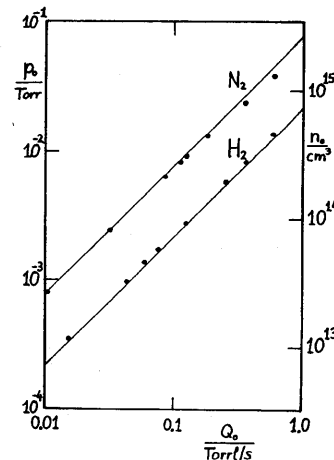


Figure 5. The measured storage cell target pressure p_0 (or atomic density n_0) as a function of the flow rate Q_0 at 8.5 mm aperture diameter. The curves represent calculations assuming molecular flow conditions.

within about a factor of two, roughly the uncertainty associated with the ion gauges. While such absolute pressure measurements provide a check for our predictions concerning the diffuse molecular gas flow through the differential pumping system, they are too inaccurate for an unambiguous measurement of the directed flow along the beam axis. To see its effect, we have measured the pressure change Δp_3 in the third chamber that results when the aperture on the left of the cell (Fig. 4) is closed from its open position to 1 mm, while keeping the gas flow into the cell constant. The results obtained with 8.5 mm aperture diameters are compared with predictions in Fig. 6, with p_0 being the cell pressure with both apertures open, i.e., at 8.5 mm. These predictions are based on the assumption that the molecules emerging from the cell aperture have a $\cos\theta$ distribution. The results for hydrogen agree within a factor of two, while for nitrogen there is a clear discrepancy which increases with p_0 . This lower than predicted beam intensity can be explained by the diffusion that the molecular beam suffers in the increasing gas density of the first chamber.

In conclusion, these first tests show that we understand the basics well enough for designing an

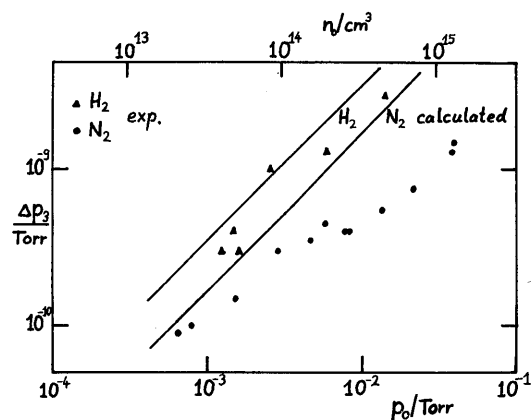


Figure 6. The pressure change Δp_3 due to the molecular beam originating from the storage cell as a function of the target pressure p_0 (or density n_0). See text for details.

actual cell target and differential pumping system. Cooling the target cell is expected to be beneficial as the gas flow, both diffuse and directed, varies with $T^{1/2}$ at constant target thickness. For experiment CE-01 a volume density n_0 of up to about $3 \cdot 10^{14}$ nuclei/cm³ should be possible with a target cell cooled to 20K. At the moment a He refrigerator cooling system is being implemented for tests of a prototype of the actual target cell.

1.2. Supersonic Jet Target

Such targets have been used mainly in low energy heavy ion nuclear physics, with a thickness typically in the range 1-100 $\mu\text{g}/\text{cm}^2$, i.e. at least about an order of magnitude thicker than we can afford. On the other hand, these targets have been used on beam lines with much less stringent vacuum requirements than we will have on the Cooler. According to calculations⁶ of axisymmetric supersonic flows it should be possible to achieve jets of a few mm diameter with a thickness in the interesting range of 10-100 ng/cm^2 and with the surrounding vacuum at a level around 10^{-5} Torr. We have started experimental testing using a set-up shown schematically in Fig. 7. Gas (H_2 or N_2) expands adiabatically through a Laval nozzle (about 0.15 mm throat diameter expanding to 1.5 mm diameter at the exit) into the high vacuum, thereby forming a supersonic jet. This jet is then removed by an intake tube, which is separated by at least 10 mm from the nozzle to provide the necessary clearance for the Cooler beam and outgoing reaction products. It is important that there is a good match of the intake tube to the jet in order to minimize the gas load into the vacuum chamber. We are now carrying out tests with a number of different nozzle/intake tube combinations. In these tests we are measuring and maximizing the fraction of the gas flow that is removed through the

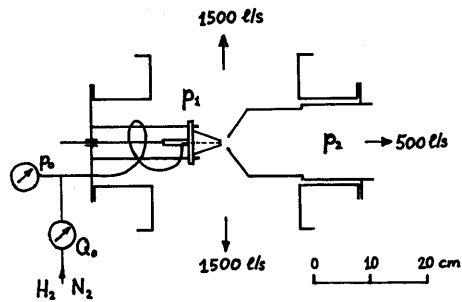


Figure 7. Schematic representation of the set-up used for tests of supersonic gas jets.

intake tube. The target thickness, which depends on the velocity of the jet gas, can only be estimated at the present time: measurements, using nuclear scattering of known cross-sections, are necessary. A test station for this purpose, using the injector Cyclotron beam, is currently in the planning stage.

2. Microparticle Target

A promising method to bring dust material into the target region is to produce charged microparticles and to use electrostatic forces to accelerate and focus them.^{7,8} Such targets are of interest because of the wide range of materials which are available in the form of μm size particles, the smallness of the luminous volume, and the reduced gas load. For a feasibility test at IUCF we have adopted the scheme used by Shelton⁹. The apparatus, shown in Fig. 8, has three stages. In the lower stage (A) the particles are contact-charged and accelerated. Emerging particles are then focused by einzel lenses (B). The proper focusing voltage has been estimated by the program EGUN,¹⁰ which calculates the trajectories of charged particles moving in a space region with an electric field distribution determined by given potentials V_1 on the electrodes (see Fig. 9). Experimentally we could see an increase in the rate of emitted particles when we changed the electrode voltages from the configuration a) to b) (Fig. 9). The upper stage (C)

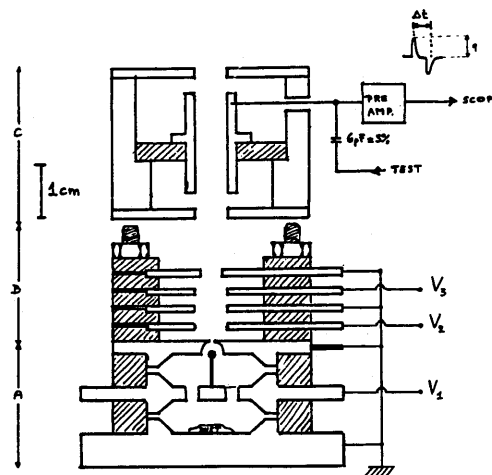


Figure 8. The "dust gun" (see text for details).

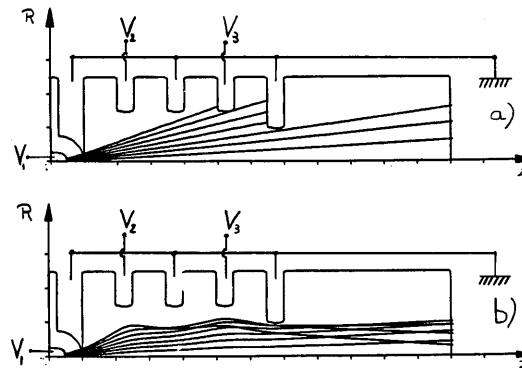


Figure 9. Calculation, by the computer program EGUN, of the dust particle trajectories for different voltages in the lens system. The boundary conditions are representing (in cylindrical coordinates R, Z) parts A and B of Fig. 6.

- a) $V_1 = 4\text{kV}$, $V_2 = V_3 = 0\text{V}$
- b) $V_1 = 4\text{kV}$, $V_2 = 5\text{kV}$, $V_3 = 3.5\text{kV}$

is a detection system. The particles pass through a cylindrical conductor connected to a high-impedance preamplifier (home-built). Observing the output signal we can deduce the charge and velocity of the particles (Fig. 10). We found them in satisfactory agreement with calculations⁷ assuming spherical particles of $10\mu\text{m}$ radius. However, the counting rate was much smaller than what would be expected assuming non-interacting particles between the charging plates. Clearly, this

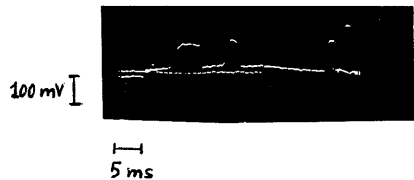


Figure 10. Example of scope signal observed with the set-up shown in Fig. 8.

assumption is not realistic. In fact, even considering only the geometrical cross-section of the particles, the mean free path length is estimated to be on the order of a few mm for a typical amount of some 30 mg of dust between the plates. Coulomb forces make the effective cross section even larger. In a two-particle encounter one would expect the exchange of charge. Since the emission volume is filled with particles of either charge one would expect a significant fraction of the particles carrying less charge than the initial value from contact charging. This explains the observation that most of the emerging dust particles had just enough energy to settle around the hole of the upper charging plate when there was no field in the lens region (Fig. 8). Only a small fraction of the particles are accelerated through the full potential given by the electrodes. We are now modifying the charging and accelerating device, trying to increase the fraction of high velocity particles.

The detection system shown in Fig. 8 is limited to particle rates of the order of 100 Hz because only particles spatially separated by more than the length of the cylindrical conductor can be counted individually. In order to overcome this limitation, we intend to measure the number density of the dust particles by Mie scattering of laser light.¹¹ The basic optical components are shown in Fig. 11. The output beam from a 25 mW Ar-ion laser is first transmitted through a spatial filter consisting of converging lens L_1 , and a pinhole aperture (PA) which

removes the noise from the laser radiation and produces a spherically expanding wave front free of intensity variations. A second lens (L_2) produces an expanded laser beam which is then focussed by lens L_3 onto the reaction volume (RV). Dust particles crossing the reaction volume will create a light flash due to Mie scattering. This light is then collected by the dublet lens system onto a photomultiplier. The primary laser beam unscattered by dust particles is deflected by a mirror into a conical beam stop (BS). In front of the photomultiplier is an adjustable aperture (A). Its opening lies safely in the shadow of the light scattered from optical components upstream cast by the deflecting mirror.

The design parameters of this optical system have been calculated and the components purchased. Machine-shop drawings for the holders of the various components are presently being made.

3. Fiber and Foil Strip Targets

3.1. Carbon Fibers

The investigation of argon-glow discharge thinned carbon fibers was continued in 1986. As expected, the new television system for the 1000 \times microscope was the analytical instrument to guide the development.

Non-uniformities in the initial thickness of the 7 μ m commercial fibers were discovered to be a cause of variations in thickness along the length (after thinning) as large as 0.7 μ m. Commercial 10 μ m fibers (Stackpole Corporation) were found to be better starting material.

Several thinning trials were conducted with different configurations of shields for the fiber/frame connection points in attempts to either increase the length of that section of the fiber which was less than 2 μ m diameter, or to decrease highly localized attack of the fiber (from argon plasma). To date, the longest



Figure 11. Schematic representation of the optical system to be used for measuring the density of microparticle targets (see text for details).

thinned section of a fiber to exhibit a diameter below $2\ \mu\text{m}$ is 6 mm in length.

3.2. Foil Strips

Foil strips are a newly developed approach to the production of fiber-like objects. The method involves the vacuum deposition of material on a substrate that is masked with a fine wire grid. Such strips are very interesting for the following reasons: first, they can be made from any isotope accessible to conventional vacuum evaporation techniques, second, since they are made in-house, they would be readily available, third, strips are expected to be stronger and more flexible than fibers, and therefore easier to handle.

Vacuum-evaporated carbon foil strips of $20\ \mu\text{g}/\text{cm}^2 \times 35\ \mu\text{m}$ wide $\times 30\ \text{mm}$ long were produced. The strips were evaporated onto a glass slide through a grill of $50\ \mu\text{m}$ diameter wires which are separated by approximately $35\ \mu\text{m}$. The strips could be floated collectively in water and picked up individually from an end with the aid of a stiff $50\ \mu\text{m}$ wire attached to a stirring stick. Precise mounting of a strip was accomplished by bringing a frame prepared with adhesive into contact with the strip before the trailing end of the strip was pulled from the water.

We also found that the strips could be pulled from the water with the trailing end totally free. A piezo-electric anti-static device was used to demonstrate the strength and flexibility of the strips as well as the ability to position them in any

direction with an appropriate electric field. The thickness, width and length of the strips achieved so far with this technique are not expected to be the limiting values. Their cross-sectional area is already nearly that of $2\ \mu\text{m}$ fibers, considered small enough to be used as internal targets. Carbon strips may also provide supports for other vacuum evaporated isotope targets as thin as desired.

3.3. Carbon Stripper Foils for Stripping Injection

Carbon stripper foils of $6\text{--}16\ \mu\text{g}/\text{cm}^2 \times 31\ \text{mm} \times 14\ \text{mm}$ with a free edge (without reinforcement) of $31\ \text{mm}$ length were developed and mounted. The method which evolved has many steps, some of which may not be essential to producing good films. Because a large number of these foils may be needed, forthcoming development work will enable us to explore the "bounds" of the recipe.

The films mounted in the last weeks of the year are far better than were hoped possible. In-beam survival tests with these foils and the strip targets are planned for early 1987.

- 1) H.-O. Meyer, Proc. CEBAF Workshop, Newport News, June 3-7, 1985, p. 503.
- 2) R.E. Pollock, Spokesman, IUCF proposal 84-112.
- 3) H.-O. Meyer et al., pg. 122 of this report.
- 4) H.-O. Meyer, Spokesman, IUCF proposal 84-113.
- 5) P.P. Singh, Spokesman, IUCF proposal 86-115.
- 6) D. Shapira and F. Sperisen, Feasibility Study for a Supersonic Gas Jet Target Facility at the IUCF Storage Ring, unpublished report, August 1986.

- 7) C.D. Hendricks, Chap. 4 in *Electrostatics and its Applications*, ed. A.D. Moore (1973).
- 8) A.Y.H. Cho, *J. Appl. Phys.* 35, 2561 (1964).
- 9) H. Shelton et al., *J. Appl. Phys.* 31 1243 (1960).
- 10) EGUN-The SLAC Electron Optics Program, W.B. Herrmannsfeldt (1981).
- 11) G. Mie, *Ann. Phys.* 25, 377 (1908); H.C. Van de Hulst, *Light Scattering by Small Particles*, John Wiley & Sons, New York, 1957.

Status of the first Cooler experiments, CE-01 and CE-02 - H.O. Meyer

The setup for experiment CE-01 is shown in Fig. 12. The purpose of the apparatus is to detect in coincidence the two outgoing protons from the near-threshold reaction $p+p+\pi^0$. Energy and angle resolution must be sufficient to completely determine the kinematics of the event. The experiment will be mounted in straight section G of the Cooler ring. The beam passes an internal gas target (T, in Fig. 12). Reaction products exit through a thin steel foil (F) and pass a 1 mm thick scintillator (S1), a flight distance, an s-y multiwire chamber WC), a 12 mm thick scintillator (DE) for dE/dx information and stop in a 100 mm thick scintillator (E) which is followed by another 12 mm thick scintillator (V) designed to veto more penetrating particles. All detectors in the stack are rotationally symmetric around the beam line. Their distance along the beam can be varied in order to choose the range of reaction angles covered from 3-18 degrees at the closest to 1-6 degrees at the farthest position. All scintillators are divided into eight symmetrical sectors in order to measure separately the energy of the two protons and to derive the multiplicity of the event for the fast trigger. The wire chamber contains an x and a y plane of wires 6.3 mm apart supplemented by one or two additional

planes at 45 degrees needed to resolve multiple-hit ambiguities.

At the moment (Jan. 1987) not all parameters of the planned detection system have been frozen. This will be possible only after the performance characteristics of prototypes of crucial elements will have been investigated experimentally. These test are currently in progress. As an example, the energy and time resolution and the light collection efficiency of one of the large volume elements of the (E) detector have been investigated using parasitic beam in the gamma cave. The resulting parameters will be used in a Monte-Carlo mockup of the full experimental setup.

The experimental information to be processed thus consists of signals from 32 photomultipliers and from the wire chambers (510 wires, with single-wire readouts). For reasons of efficiency and economy the step to ECL-type electronics will be made, thus putting all of the data acquisition, including the definition of the fast trigger, under computer control. This represents a departure from the hardwired logic used in most IUCF experiments so far. A CAMAC interface and a dedicated microVAX computer will complete the system, making data acquisition electronics autonomous and allowing extensive testing prior to the actual running of the experiment. Orders have been placed for a large fraction of the electronics and the computer system. This equipment will also form the basis for implementing subsequent experiments in the Cooler building.

In planning for this experiment attention has been given to being able to share as much of the hardware with CE-02, the second Cooler experiment to be run around the middle of 1988. The goal of this experiment is to detect the formation of pionic atoms as a

all aspects of the first two Cooler experiments has been started. A local Cooler Experimental Group has been constituted and responsibilities for parts of the design work have been taken over by individuals.

Tests of Position Sensitive Neutron Counter for Experiment CE-03 - W.W. Daehnick, C.C. Foster, P.C. Li, and S.K. Saha

In preparation for the pp-pn Cooler experiment CE-03, a position sensitive neutron detector was designed, and a prototype section was tested. The completed neutron detector will consist of an array of ten to twelve bar-shaped plastic scintillators, each of the dimension 120 cm \times 15 cm deep \times 5 cm high as shown in Fig. 13. By construction, the vertical resolution is 5 cm and the horizontal resolution should be 5 cm, or better if possible. The neutron detector array will be preceded by a thin 120 cm \times 60 cm scintillator run in anti-coincidence to prevent the detection of charged particles. The horizontal position measurement is accomplished by charged particles. The horizontal position measurement is accomplished by timing the arrival of the light signal at the left photo-multiplier versus the delayed signal from the right photo-multiplier.

A single section prototype of the anticipated dimension was initially tested by S. Saha with the Pittsburgh Van de Graaff Beam. Tests with collimated 10 MeV protons resulted in resolutions of $\Delta_x = 4.8$ cm, and use pp-pn π experiment, typical neutron energies would exceed 70 MeV with a corresponding increase in light intensity; however, the recoil protons resulting from the incident neutrons are not co-linear and have a transverse range of about 2 cm. In addition, in the real experiment, considerable background from gamma rays and multiplyscattered neutrons is expected leading to a very high instantaneous counting rate. Neither of

these conditions could be duplicated in the Pittsburgh test runs.

At low energies, the use of dual photomultipliers at each end of the scintillator bar gave significant improvement in uniformity of light collection and resolution. The tests at Indiana also aimed at determining the need for this light collection.

IUCF runs at 100 MeV with elastic and inelastic protons (i.e. protons from a Lithium foil) yielded a fwhm resolution of 2.7 cm for a threshold setting at about 10% of the maximum proton energy. The horizontal range of the accepted protons was determined by a 1 cm wide ΔE detector mounted directly in front of the 1.2 m long bar. A fast coincidence totally suppressed background at other areas of the detector, even for measurements with instantaneous counting rates of the order of 3×10^5 per second. Position indication was of good linearity, with the exception of regions of about 5 cm, or less, from the ends.

Energetic neutrons were generated by the Li(p,n) reaction. Since collimation by coincidence was not practical for neutrons, a 2 meter deep collimator with an opening of about 40 mm height and 20 mm width was interposed, and the rest of the detector was shielded by lead bricks. The collimator was rotated in order to

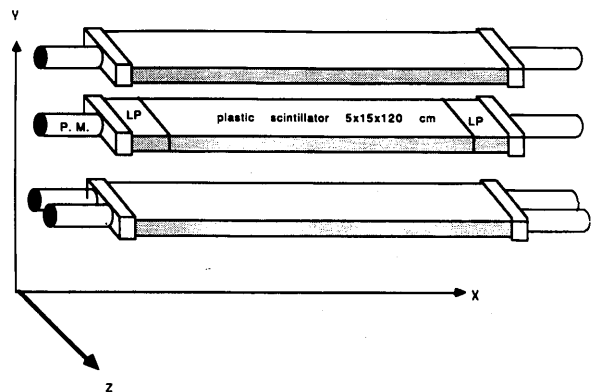
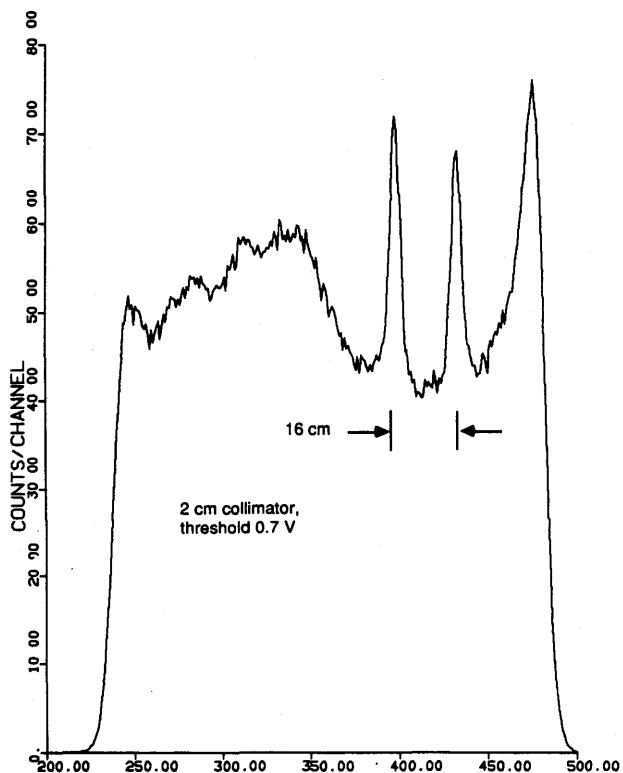


Figure 13. Sketch of prototype neutron detectors

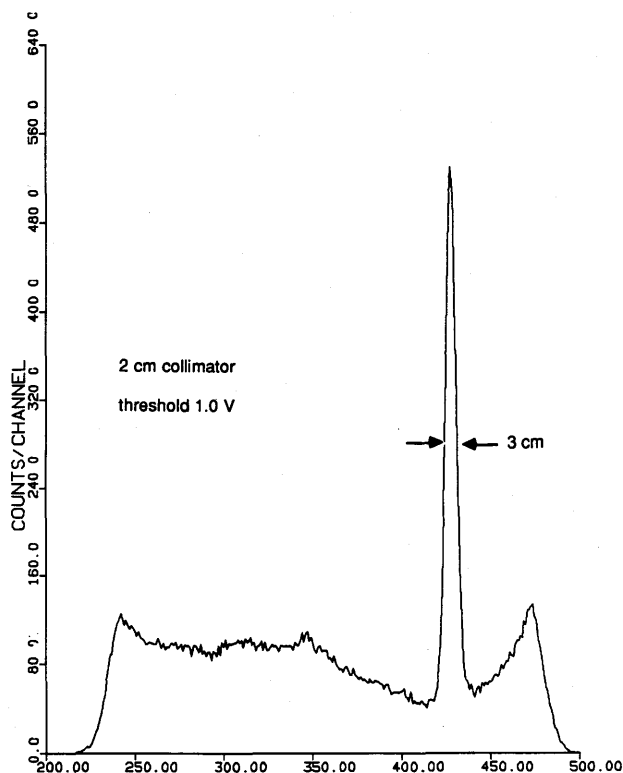
illuminate (sequentially) two different spots of the detector, 16 cm apart. The resulting spectrum is illustrated in Fig. 14. A resolution of 3.1 cm was obtained. A change in the threshold setting from 10% (shown) to 15% did not significantly effect the resolution setting for collimated neutrons, but resulted in a rapid decrease of the detected continuous background as shown in Fig. 15. In the $pp\text{--}pn\pi$ experiment, the background will be totally eliminated by multiple coincidence requirements whereas the neutron resolution should be retained at about the level found. If the finite size of the collimated aperture is unfolded from the observed peak, an intrinsic resolution of about 2.4 cm is obtained for the current design.

The switch from the use of four photomultipliers to two photomultipliers per bar resulted in no measurable deterioration of position resolution at 100 MeV. However, the previously observed non-linearity close to the ends increases. With light detection by two photomultipliers at each end, the light intensity as a function of position was nearly uniform throughout detector volume up to 30 cm from the closest end from where it began to rise by as much as 15%. For light detection with a single photomultiplier, an increase of light intensity became noticeable 50 cm from the end, increasing to a peak of about 43% above average at the 18 cm position. We plan to counteract this light collection and non-linearity effect with light pipe extensions of the scintillator bar so that the



IUCF: TIME SPECTRUM OF NEUTRON DETECTOR RUN# 3033.

Figure 14. Position spectrum obtained for sequential exposures with rotated neutron collimator.



IUCF: TIME SPECTRUM OF NEUTRON DETECTOR RUN# 3028.

Figure 15. Spectrum with single collimator setting and increased threshold.

detection of neutrons will occur at least 20 cm away from the photomultiplier cathodes.

The scintillating material used was the NE110 Bicron equivalent, which has a low self absorption. For the anticipated placement, 7 m from the target, the

intrinsic (horizontal) angular resolution of the neutron detector corresponds to $\Delta\theta = 0.2$ degrees. This accuracy is safely within the limits required by the experiment.